6th CIRP Conference on Surface Integrity

Analysis of chip segmentation frequencies in turning Ti-6Al-4V for the prediction of residual stresses

Florian Pachnek[a],*, Germán González[a], Daniel Diaz Ocampo[b], Michael Heizmann[b], Frederik Zanger[a]

[a]*wbk Institute of Production Science, Karlsruhe Institute of Technology (KIT), Kaiserstr. 12, 76131 Karlsruhe, Germany*
[b]*Institute of Industrial Information Technology (IIIT), Karlsruhe Institute of Technology (KIT), Hertzstr. 16, 76187 Karlsruhe, Germany*

* Corresponding author. Tel.: +49-721-608-42455; fax: +49-721-608-45004. *E-mail address:* florian.pachnek@kit.edu

Abstract

Machining-induced residual stresses depend on the process parameters and are strongly influenced by the tool wear. The chip segmentation frequency in turning of Ti-6Al-4V can be obtained by processing signals of acoustic emission (AE) caused by the cutting process and used to estimate the tool wear condition. In this work, chip segmentation frequencies during longitudinal turning of Ti-6Al-4V are measured using AE sensors and correlated with the process parameters, abrasive tool wear and residual stresses. The resulting models allow for predition of significant characteristics in the residual stress distribution based on in-process measured chip segmentation frequencies.

Keywords: turning; acoustic emission; residual stress

1. Introduction

Residual stress states of high-performance components have a significant influence on the resulting fatigue strength [1,2]. Selecting machining parameters for achieving compressive residual stresses in the subsurface is still challenging [3]. Previous studies showed a negative impact of tool wear on surface integrity due to higher thermal loads leading to increased tensile residual stresses [4]. Severe tool wear increases thermo-mechanical load at the shear zone and leads to segmentation frequency variations, as shown by Zanger et al. during orthogonal cutting of Ti-6Al-4V [5]. Wu et al. [6] established a numerical model to identify correlations between residual stress profiles and chip segmentation frequency in orthogonal turning of Ti-6Al-4V, however the research lacks on experiments and the effect of tool wear was not considered. Liang et al. [7] proposed an analytical model for predicting the influence of tool wear on the residual stress distributions, neglecting the chip shape. Modeling of residual stresses

distributions in face turning and surface stresses in longitudinal turning of Ti-6Al-4V was conducted in previous studies, however the relationship with the chip segmentation frequency was not investigated [8,9]. González et al. [10] showed variations in chip segmentation frequency with process parameters and tool wear in longitudinal turning and proposed techniques to identify chip segmentation frequencies in-process using acoustic emissions (AE).

In this work, longitudinal turning of Ti-6Al-4V is performed under different cutting speeds and flank wear states. AE sensors and optical chip analyses are used to identify chip segmentation frequency and its dependence on thermo-mechanical loads and tool wear. The residual stress depth distributions in the subsurface of the workpieces are also measured. Characteristics of the resulting residual stress profiles are correlated with the associated chip segmentation frequency. An AE-based model for the prediction of residual stress is proposed. This model estimates residual stress profiles using the tool wear state, the process parameters and the chip segmentation frequency.

Nomenclature

v_c	Cutting speed, m/min
f	Feed, mm/rev
a_p	Cutting depth, mm
f_{cs}	Chip segmentation frequency, kHz
α	Clearance angle, °
κ_r	Tool cutting edge angle, °
γ	Rake angle, °
VB	Flank wear, µm
N	Number of inverted zero-crossings
Δs	Average peak-to-peak distance, µm
σ_{surf}	Surface residual stress, MPa
σ_{min}	Minimum residual stress, MPa
d	Depth under workpiece surface, µm
d_0	Impact depth of compressive residual stress, µm
$d_{\sigma,min}$	Depth of minimum residual stress, µm

2. Setup and method

2.1. Experimental setup

Longitudinal turning tests were conducted on a vertical turning machine Index V100 under dry conditions. Uncoated carbide inserts CCMW120404 with a cutting edge radius of 50 µm were placed in a tool holder providing a tool cutting edge angle κ_r of 75°, a rake angle γ of 0° and a clearance angle α of 7°. A three component dynamometer type 9257B from Kistler beneath the holder measured the process forces. In order to capture the chip segmentation frequencies, a piezoelectric AE sensor VS45-H from Vallen Systeme was mechanically mounted on the tool holder in the cutting direction as shown in Fig. 1. The raw signal from the AE sensor is processed by an AE-preamplifier before being recorded by a PXI station. The duration from in-process measurement to data acquisition and processing is estimated to be between 10 and 100 ms.

The process parameters are listed in Table 1. Cutting speeds were varied using a new insert after each cut. At a cutting speed of 120 m/min, abrasive flank wear was identified as the dominant wear mechanism, while slower v_c lead to adhesion and more aggressive v_c caused crater and notch wear on the rake face. In order to investigate the separate influence of flank wear on the chip segmentation frequency and residual stresses a fixed cutting speed of 120 m/min was chosen. The flank wear was produced by additional cutting tests and characterized by repeated measurements with an optical light microscope until the desired values were reached. Each cut was conducted on a separate section of the workpiece, as residual stress measurements followed the turning process.

Table 1. Process parameters for longitudinal turning tests

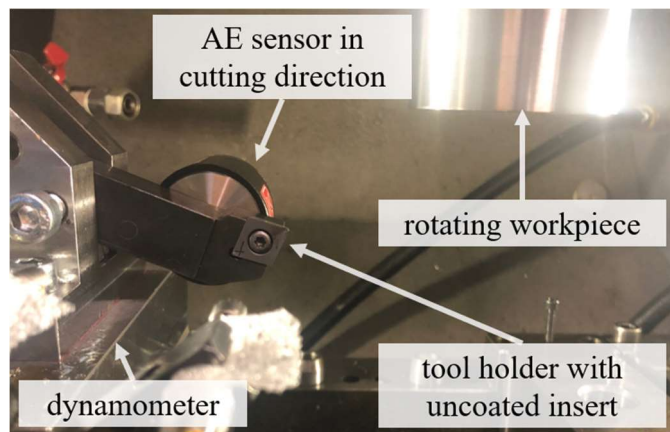| v_c m/min	a_p mm	f mm/rev	κ_r °	γ °	α °	VB µm
120; 200; 300	0.3	0.2	75	0	7	0; 100; 200

Fig. 1. Experimental setup for longitudinal turning tests.

2.2. Chip segmentation frequency analysis

The segmentation frequency of the produced chips can be evaluated using AE processing techniques or optical chip analysis. Both options were applied using the methods developed and presented in previous studies [10,11]. During machining, AE signals in sawtooth waveform shown in Fig. 2 (a) are generated, caused by the periodic cutting forces during segmented chip formation. The strongly inharmonic raw data was evaluated by inverting the time interval between successive zero crossing points resulting in a frequency. Plotting the number of inverted intervals N as a histogram with unequally spaced bins allows for estimating the chip segmentation frequency during the turning process as shown in Fig. 2 (b). In addition, chip segmentation frequencies were directly obtained by optical chip analysis.
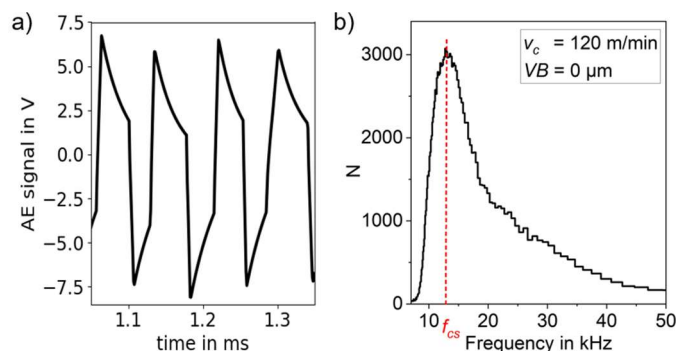

Fig. 2. (a) AE signals in saw tooth waveform during the cutting process; (b) Histogram obtained from AE data processing.

This allows the verification of the AE signal processing methods. After each experiment, chips were collected and evaluated using a confocal laser scanning microscope to measure the average distance Δs between two consecutive segmentation peaks presented in Fig 3. As the chips are getting compressed during the cutting process an additional compression factor, depending on the weight and length of the examined chip segments, was considered [12].
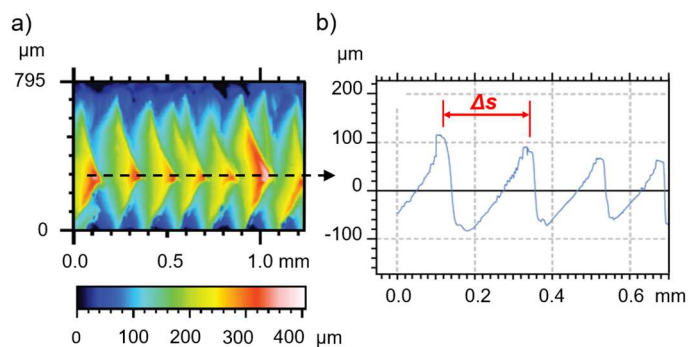
Fig. 3. (a) Optical chip analysis for measuring; (b) average peak-to-peak distance Δs.

2.3. Residual stress analysis

The residual stress analysis on the machined Ti-6Al-4V samples in tangential and axial direction were performed using the sin^2-ψ-method and a four-circle diffractometer in ψ-geometry. Ni-filtered CuKα type radiation was used. The measurements were performed at 15 different angles in the range $-60° \leq \psi \leq 60°$ over the vertical with an equidistant step size. The stress analyses were evaluated assuming isotropic material behavior with the radiographic values $E = 113000$ MPa for the elastic modulus and $\nu = 0.32$ for the Poisson's ratio. Depth profiles of residual stresses were generated by electrochemical ablation of the surface and repeated measurements.

3. Results and discussion

3.1. Chip segmentation frequency

The results of AE signal processing and optical chip analysis differ from each other, caused by high measurement uncertainties in determining the compression factor used in optical chip analysis or distorted AE signals due to reflections inside the tool holder. Fig. 4 (a) shows increasing chip segmentation frequencies for higher cutting speeds. The error bars indicate the standard deviation from three replicate tests and are very small as the results are well reproducible and the general trend is the same in both methods.
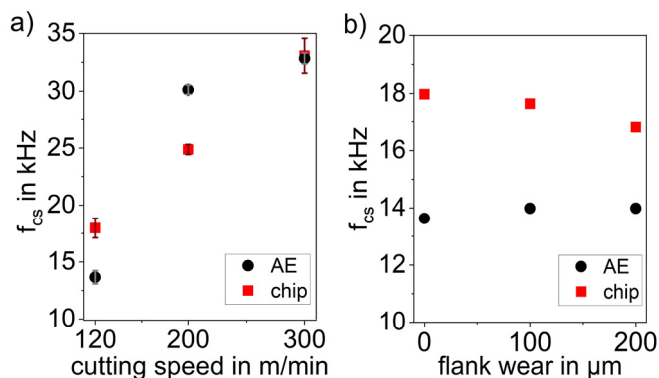

Fig. 4. Chip segmentation frequencies from optical chip analysis and AE-processing under (a) varying cutting speeds; (b) progressing flank wear at $v_c = 120$ m/min.

The experimental results using tools with progressing flank wear are shown in Fig. 4 (b). Statistical information is not provided as identical tool wear conditions are hard to reproduce and therefore no tests were exactly replicate. The estimated chip segmentation frequency only changes slightly. This trend is validated using the optical chip analysis, where only a minor decrease is notable. Both the AE-based method and the optical chip analysis have high uncertainties, so that the minor trends are not meaningful nor interpretable. The frequencies remain at the same range with increasing flank wear. A systematic difference of 2.8 to 4.3 kHz between optical chip and AE analyses is present.

3.2. Residual stress distributions

The residual stress depth distributions were measured in tangential direction and axial direction, as shown in Fig. 5 (a) and 5 (b) respectively. The stresses in the axial direction are substantially more affected by the higher cutting speeds than the tangential stresses. Higher compressive residual stresses are generated in the subsurface in axial direction due to the machining process. In axial direction higher cutting speeds cause significant change in the surface stress from minimal tensile stresses at 120 m/min cutting speed to a compressive stress of 720 MPa at 300 m/min. The maximum compressive stress in the subsurface increases by 90 %. Additionally, the depth at which the maximum compressive value occurs as well as the overall impact depth of the machining process are shifted deeper into the workpiece. Concerning the residual surface stress in tangential direction there is no clear tendency, as illustrated in Fig. 5 (b), but values move into the tensile area with increasing cutting speed. The peak compressive stresses are at a similar level, but their occurrence is deeper under the surface with increasing cutting speed. The impact depth of the compressive stresses increases significantly and is comparable to the results in axial direction. Additionally, an increasing difference between the residual stress distribution in axial and tangential direction is present due to the cutting speed variation. The higher cutting temperatures due to increased cutting speeds only seem to have an impact on the tangential surface stress as higher tensile stresses were measured. For these process parameters, the results suggest that the hardening through mechanical loads outweighs the increased temperatures and their effect on the residual stress distribution. Fig. 6 shows the residual stresses at a fixed cutting speed of 120 m/min comparing new cutting edges to tools with flank wear of approximately 100 μm and 200 μm. Increasing tool wear increases the depth effect of residual compressive stresses in the subsurface, both in axial and in tangential direction. The surface value in axial direction does not follow a clear trend, while the value in tangential direction moves from compressive to tensile stress with increasing wear. Compared to Fig. 5 the influence of abrasive flank wear is low and clear tendencies with increased wear condition are hard to identify, as results do not differ significantly. The evaluation of the force signals using a new insert shows an increase of the mean passive force from 90 N to 150 N at a flank wear of 100 μm.
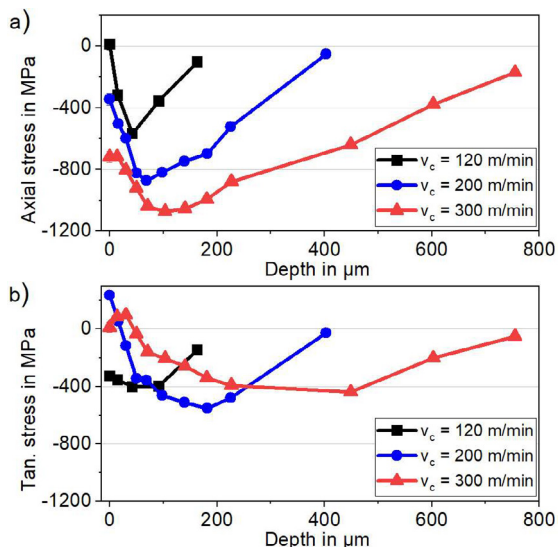
Fig. 5. Residual stress distributions in the subsurface in (a) axial direction and (b) tangential direction at varied cutting speeds

3.3. Correlations with chip segmentation frequencies

These experiments show that changes in thermo-mechanical loads due to cutting speed variations and growing abrasive tool wear result in varying residual stress distributions. As residual stress measurements cannot be performed during machining, correlations to in-process measurable variables, as chip segmentation frequency, must be established. In this work only the influence of abrasive tool wear is studied, which does not lead to significant changes in segmentation frequency, wherefore tool wear is not included in the models yet. As depth profiles are hard to describe, the residual stress state is decomposed into representative characteristics. Those are the surface value σ_{surf}, the minimum stress σ_{min}, its depth under the surface $d_{\sigma,min}$, and depth of impact d_0 as shown in Fig. 7. These representative characteristics can be correlated with the segmentation frequency using linear functions type $\sigma = A + B \cdot f_{cs}$. Separate models were developed using the frequencies identified by optical and AE-based strategies and compared with each other.

Further increased wear of 200 µm leads to a passive force of 190 N. Cutting forces only increase about 14 % compared to a new insert. It was to be expected that the increased force would lead to an increase in residual compressive stresses. At the same time, the increased contact zone between workpiece and the worn tool's flank face leads to additional friction and therefore rises in workpiece temperatures. At the surface, the increased friction heat results in more tensile stresses as stated by Chen et. al [4]. However, this can only be confirmed for the tangential stress as axial surface stresses tend to be more compressive with worn tools. In the subsurface the opposing mechanical and thermal effects on the residual stress state seem to balance each other out for the most part as the depth profiles do not differ much. Only the impact depth of compressive stresses increases clearly with flank wear.

Fig. 7. Extracted characteristics from residual stress depth distributions.

For the axial direction, the fitted curves for varied cutting speeds are shown in Fig. 8 with the function coefficients listed in Table 2, with the indices of A and B indicating which frequencies were used. All four characteristics of the residual stresses correlate almost exactly linearly with the frequencies obtained by optical chip analysis. However, for predicting the stress in-process the AE frequency must be used. The models show the same tendency, but the quality of the linear fit decreases as shown by the lower Pearson correlation coefficients R_{AE} and R_{chip} in Table 2. The identified gradients and therefore the dependence of the stress characteristics on the frequency are slightly smaller. This can be seen when comparing the function gradients B_{AE} and B_{chip} in Table 2. Analogous models for stress characteristics in tangential direction are illustrated in Fig. 9 with their parameters listed in Table 3. Modeling the depths $d_{\sigma,min,tan}$ and $d_{0,tan}$ using the linear approach results in good correlations as the associated R values in Table 3 indicate. The stress characteristics $\sigma_{surf,tan}$ and $\sigma_{min,tan}$ do not increase monotonously with higher cutting speeds.
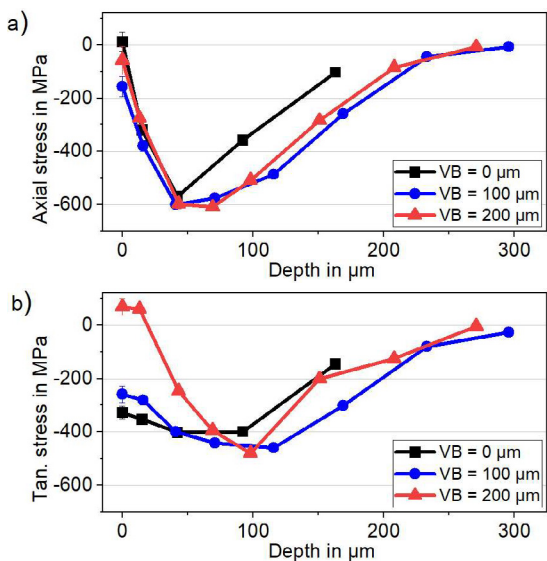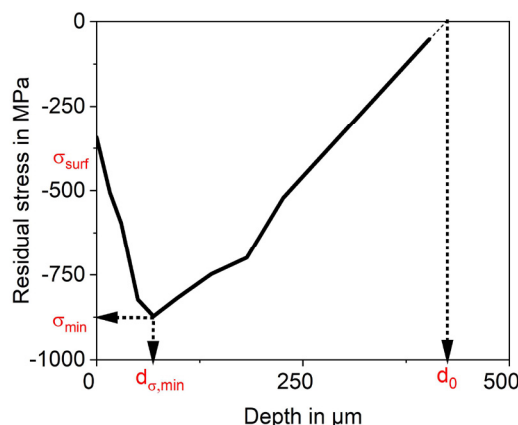

Fig. 6. Residual stress distribution in the subsurface under progressing flank wear at $v_c = 120$ m/min in (a) axial direction and (b) tangential direction.
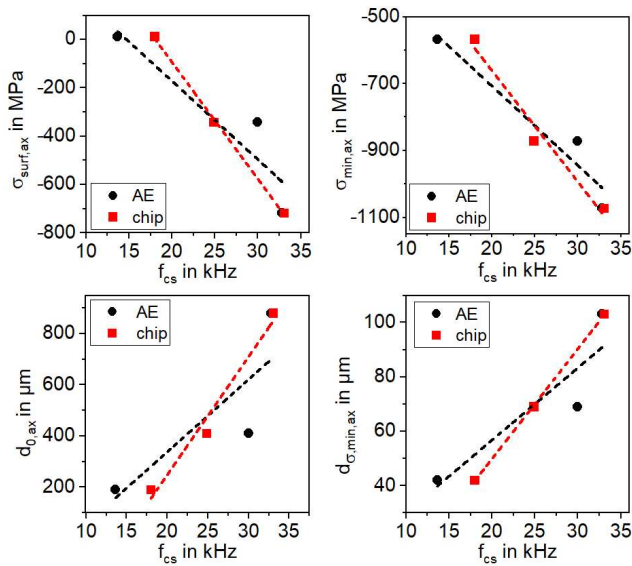
Fig. 8. Chip segmentation frequency based modeling of residual stress state characteristic in axial direction under different cutting speeds using unworn tools.

Table 2. Parameters and correlation coefficients for modeling axial stress characteristics with chip segmentation frequencies.

Parameter	A_{AE}	B_{AE}	R_{AE}	A_{chip}	B_{chip}	R_{chip}
$\sigma_{surf,ax}$	476.8	-0.032	-0.919	871.9	-0.048	-0.999
$\sigma_{min,ax}$	-233.6	-0.024	-0.964	2.2	-0.033	-0.986
$d_{\sigma,min,ax}$	3.6	0.003	0.899	-31.0	0.004	1.000
$d_{0,ax}$	-226.8	0.028	0.829	-672.9	0.046	0.988

A local minimum respectively maximum of the three measurement points is present at v_c = 200 m/min and the associated chip segmentation frequencies. A linear model is therefore not suitable to correlate those characteristics. Establishing more complex models based on quadratic functions is possible, but should based on more than three points to make sure that a local extreme point is actually present. For reliable modeling, discrepancies between chip segmentation frequencies obtained by AE data processing and optical methods need to be minimized. This can be done by optimizing the positioning and mounting technique of the AE sensors to minimize reflections inside the toolholder as well as improving the AE data processing methods. These models can be used to predict characteristics of the resulting residual stress distributions based on the in-process measurable chip segmentation frequency, and therefore enable the configuration of a desired residual stress state by adjusting the process parameters accordingly.

3.4. Correlations with flank wear

As stated above, no significant changes in segmentation frequency are observable for progressing abrasive tool wear. The changes in the residual stress characteristics with increasing flank wear are shown in Fig. 10.
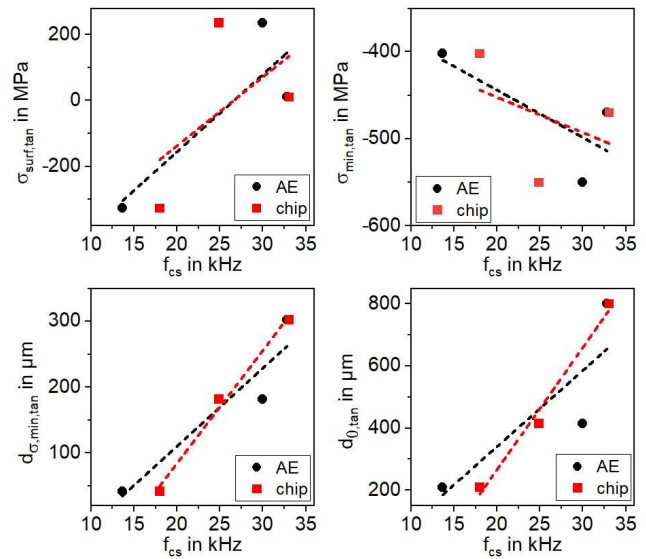

Fig. 9. Chip segmentation frequency based modeling of residual stress state characteristic in tangential direction under different cutting speeds using unworn tools.

Table 3. Parameters and correlation coefficients for modeling tangential stress characteristics with chip segmentation frequencies.

Parameter	A_{AE}	B_{AE}	R_{AE}	A_{chip}	B_{chip}	R_{chip}
$\sigma_{surf,tan}$	-624.5	0.025	0.856	-554.3	0.021	0.556
$\sigma_{min,tan}$	-335.0	-0.005	-0.761	-371.2	-0.004	-0.414
$d_{\sigma,min,tan}$	-126.8	0.012	0.942	-258.7	0.017	0.991
$d_{0,tan}$	-149.9	0.025	0.846	-520.6	0.039	0.992

For better visibility the points are connected with dotted lines to identify direct correlations with the wear state. The only characteristics that can be clearly assigned to increasing wear are the surface stress in tangential direction $\sigma_{surf,tan}$, the maximum compressive stresses $\sigma_{min,ax}$ and $\sigma_{min,tan}$ and the depth $d_{\sigma,min,ax}$.
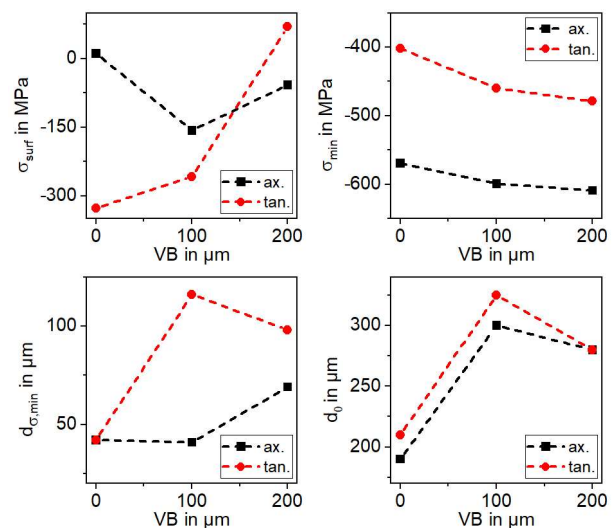

Fig. 10. Residual stress characteristics under different tool wear conditions at v_c = 120 m/min.

The minimum stresses decrease slightly, but the surface tangential stress correlates significantly with tool wear. The other four characteristics have a local extremum, which is difficult to interpret due to the small amount of measurement points. Therefore, no analytical models were established. The results show that abrasive wear only affects few residual stress characteristics. No significant change in the chip segmentation frequency was observed using worn tools. Therefore, no link between pure abrasive flank wear and the segmentation frequency was identified in this experimental setup. However, the wear did lead to changes in the residual stress distribution. This means it is not sufficient to consider pure abrasive flank wear, even if first good correlations have been found in this study. Previous turning tests showed altered segmentation frequencies with other wear mechanisms such as adhesion, crater and notch wear and their combined occurrence with abrasive wear [10]. Their effect on the resulting residual stresses in the subsurface must therefore be investigated in future studies.

4. Conclusions

In this work longitudinal turning tests of Ti-6Al-4V under different cutting speeds and flank wear conditions were performed. Acoustic emissions of the machining process were recorded and evaluated leading to an estimated value of the chip segmentation frequency. The resulting residual stress state in the machined samples were measured using X-ray diffraction and modeled using the chip segmentation frequency. Following conclusions can be drawn:

- Chip segmentation frequency increases with higher cutting speeds
- Increased cutting speeds lead to more compressive residual stresses in the subsurface, but have different effects on the stresses in tangential and axial direction.
- Correlations between significant characteristics of the residual stress profile and the in-process measured chip segmentation frequency are present, resulting in AE-based residual stress models.
- Abrasive flank wear has no significant influence on chip segmentation frequency and only a minor impact on residual stresses in the subsurface, but determine the surface values.

Reliable empirical models for the prediction of residual stresses over a wide range of process parameters, tool wear conditions and chip segmentation frequencies need a bigger data base.

References

[1] Javidi A, Rieger U, Eichlseder W (2008) The effect of machining on the surface integrity and fatigue life. International Journal of Fatigue 30(10-11):2050–5.

[2] Matsumoto Y, Hashimoto F, Lahoti G (1999) Surface Integrity Generated by Precision Hard Turning. CIRP Annals 48(1):59–62.

[3] Jawahir IS, Brinksmeier E, M'Saoubi R, Aspinwall DK, Outeiro JC, Meyer D, Umbrello D, Jayal AD (2011) Surface integrity in material removal processes: Recent advances. CIRP Annals 60(2):603–26.

[4] Chen L, El-Wardany TI, Harris WC (2004) Modelling the Effects of Flank Wear Land and Chip Formation on Residual Stresses. CIRP Annals 53(1):95–8.

[5] Zanger F, Kacaras A, Bächle M, Schwabe M, Puente León F, Schulze V (2018) FEM simulation and acoustic emission based characterization of chip segmentation frequency in machining of Ti-6Al-4V. Procedia CIRP 72:1421–6.

[6] Wu ZR, Zhu KK, Pan L, Fang L, Song YD (2020) Investigation of the correlation between mechanical chip morphology and surface residual stress for Ti6Al4V alloy. J Mech Sci Technol 34(10):3997–4004.

[7] Liang X, Liu Z, Wang B, Song Q, Cai Y, Wan Y (2021) Prediction of residual stress with multi-physics model for orthogonal cutting Ti-6Al-4V under various tool wear morphologies. Journal of Materials Processing Technology 288:116908.

[8] Özel T, Ulutan D (2012) Prediction of machining induced residual stresses in turning of titanium and nickel based alloys with experiments and finite element simulations. CIRP Annals 61(1):547–50.

[9] Abboud E, Attia H, Shi B, Damir A, Thomson V, Mebrahtu Y (2016) Residual Stresses and Surface Integrity of Ti-alloys During Finish Turning – Guidelines for Compressive Residual Stresses. Procedia CIRP 45:55–8.

[10] González G, Schwär D, Segebade E, Heizmann M, Zanger F (2021) Chip segmentation frequency based strategy for tool condition monitoring during turning of Ti-6Al-4V. Procedia CIRP 102:276–80.

[11] Diaz Ocampo D, González G, Zanger F, Heizmann M (2021) Schätzung der Segmentspanbildungsfrequenz mithilfe von Körperschallsignalen. tm - Technisches Messen 88(s1):s37-s41.

[12] Schwär D, González G, Segebade E, Zanger F, Heizmann M (2020) Evaluation of the acoustic emission caused by the chip segmentation frequency during machining of titanium alloy. tm - Technisches Messen 87(11):714–20.